JOURNAL OF THE AMERICAN COLLEGE OF CARDIOLOGY
VOL. 69, NO. 3, 2017

ISSN 0735-1097/$36.00
http://dx.doi.org/10.1016/j.jacc.2016.10.065

AF Ablation Guided by Spatiotemporal Electrogram Dispersion Without Pulmonary Vein Isolation

A Wholly Patient-Tailored Approach

Julien Seitz, MD,[a] Clément Bars, MD,[a,b] Guillaume Théodore, MD,[c] Sylvain Beurtheret, MD,[a] Nicolas Lellouche, MD, PhD,[d] Michel Bremondy, MD,[a] Ange Ferracci, MD,[a] Jacques Faure, MD,[a] Guillaume Penaranda,[e] Masatoshi Yamazaki, MD, PhD,[f] Uma Mahesh R. Avula, MD,[f] Laurence Curel, MS,[a] Sabrina Siame,[a] Omer Berenfeld, PhD,[f] André Pisapia, MD,[a] Jérôme Kalifa, MD, PhD[f]

ABSTRACT

BACKGROUND The use of intracardiac electrograms to guide atrial fibrillation (AF) ablation has yielded conflicting results.

OBJECTIVES The authors evaluated the usefulness of spatiotemporal dispersion, a visually recognizable electric footprint of AF drivers, for the ablation of all forms of AF.

METHODS The authors prospectively enrolled 105 patients admitted for AF ablation. AF was sequentially mapped in both atria with a 20-pole PentaRay catheter. The authors tagged and ablated only regions displaying electrogram dispersion during AF. Results were compared to a validation set in which a conventional ablation approach was used (pulmonary vein isolation/stepwise approach). To establish the mechanism underlying spatiotemporal dispersion of AF electrograms, the authors conducted realistic numerical simulations of AF drivers in a 2-dimensional model and optical mapping of ovine atrial scar-related AF.

RESULTS Ablation at dispersion areas terminated AF in 95% of the 105 patients. After ablation of 17 ± 10% of the left atrial surface and 18 months of follow-up, the atrial arrhythmia recurrence rate was 15% after 1.4 ± 0.5 procedures per patient versus 41% in the validation set after 1.5 ± 0.5 procedures per patient (arrhythmia free-survival: 85% vs. 59%; log-rank $p < 0.001$). Compared with the validation set, radiofrequency times (49 ± 21 min vs. 85 ± 34.5 min; $p = 0.001$) and procedure times (168 ± 42 min vs. 230 ± 67 min; $p < 0.0001$) were shorter. In simulations and optical mapping experiments, virtual PentaRay recordings demonstrated that electrogram dispersion is mostly recorded in the vicinity of a driver.

CONCLUSIONS The clustering of intracardiac electrograms exhibiting spatiotemporal dispersion is indicative of AF drivers. Their ablation allows for a nonextensive and patient-tailored approach to AF ablation. (Substrate Ablation Guided by High Density Mapping in Atrial Fibrillation [SUBSTRATE HD]; NCT02093949) (J Am Coll Cardiol 2017;69:303–21)

Listen to this manuscript's audio summary by *JACC* Editor-in-Chief Dr. Valentin Fuster.

From the [a]Unité de Rythmologie Interventionnelle, Hôpital Saint Joseph Marseille, France; [b]Service de Cardiologie, Institut Mutualiste Montsouris, Paris, France; [c]Service de Cardiologie, CHU, Nice, France; [d]Service de Cardiologie, CHU Henri Mondor, Creteil, France; [e]Département Statistique, Laboratoire Alphabio, Marseille, France; and the [f]Center for Arrhythmia Research, Cardiovascular Research Center, Department of Internal Medicine, Division of Cardiology, University of Michigan, Ann Arbor, Michigan. The study was not funded by industry and received no financial support. Dr. Yamazaki was supported by Grant-in-Aid for Scientific Research (C) 15K09077 and Joint International Research grant 15KK0341. Dr. Seitz has received speaker fees and honoraria as a consultant from Biosense Webster; has received speaker fees from St. Jude Medical and Medtronic; and owns shares of Volta Medical. Dr. Bars has received speaker fees and honoraria as a consultant from Biosense Webster; and owns shares of Volta Medical. Dr. Theodore has received honoraria as a consultant from Biotronik, Boston Scientific, St. Jude Medical, and Medtronic. Prof. Lellouche has received speaker fees from Medtronic. Dr. Bremondy has received honoraria as study investigator from St. Jude Medical for the STAR AF II trial study. Drs. Ferracci and Faure have received honoraria from St. Jude Medical as consultants. Dr. Berenfeld has received grants and donations from Medtronic and St. Jude Medical; is a consultant for Acutus

ABBREVIATIONS AND ACRONYMS

AAD = antiarrhythmic drug
AF = atrial fibrillation
AFCL = atrial fibrillation cycle length
AT = atrial tachycardia
CFAE = complex fractionated atrial electrogram
CL = cycle length
CS = coronary sinus
IQR = interquartile range
LA = left atrial/atrium
PV = pulmonary vein
PVI = pulmonary vein isolation
RA = right atrial/atrium
RF = radiofrequency
SR = sinus rhythm
VAV = voltage absolute value

Visual appraisal of the sequence and morphology of intracardiac electrograms sufficiently guides ablation of most ventricular and atrial arrhythmias. Atrial fibrillation (AF) is an exception to this paradigm. The targeting of complex fractionated electrograms (CFAE) as stand-alone or adjunctive ablation therapy has yielded variable results (1–8). Although some have reported good results when targeting CFAEs (6–8), a growing number of reports found little advantage in targeting CFAEs after having isolated the pulmonary veins (PVs) (1–5). CFAE ablation is usually guided by recording fractionated electrograms at the tip of a single intracardiac electrode. Multiple studies have suggested that multipolar electrode-obtained CFAEs provide added value beyond single electrode-recorded CFAEs by enabling classification of CFAEs as "active" or "passive" (9–11). The authors of these studies specifically noted that fractionation occurring in a nonsimultaneous fashion at neighboring electrode locations (time dispersion) and organized in well-defined clusters (spatial dispersion) may indicate the presence of an underlying source of AF (9–12). Recently, it was suggested that such multielectrode electrogram clusters might help in guiding ablation (11,13).

SEE PAGE 322

Previously, it was shown that intracardiac electrogram analysis might enable the visualization of AF drivers (14,15). It is unclear, however, whether multipolar electrogram signatures can serve as surrogates for the presence of drivers. The purpose of this pilot study was to describe a visually recognizable intracardiac electrogram abnormality that can identify regions of AF drivers and represent effective target sites for ablation of paroxysmal or persistent AF.

METHODS

The hypothesis underlying this study is that electrograms recorded simultaneously by a multipolar catheter displaying both spatial and temporal dispersion areas are indicative of AF drivers, regardless of whether these electrograms are fractionated or not. In **Figure 1A**, we present the typical feature of abnormal multipolar electrograms associated with AF drivers: the spatiotemporal dispersion of electrical activation. **Figures 1B and 2** show examples of fractionated and nonfractionated single-bipole and multipolar electrograms recorded in dispersion regions.

Between September 2013 and July 2014, 126 patients with drug-refractory symptomatic AF were prospectively enrolled at 3 centers (Hopital St-Joseph, Marseille; Institut Mutualiste Monsouris, Paris; and Centre Hospitalier Universitaire, Nice). Ablations were performed independently by 7 electrophysiologists. The validation set included a cohort of patients with symptomatic drug-refractory AF who underwent ablation using a conventional approach. From a database of 98 patients ablated conventionally (pulmonary vein isolation [PVI]/stepwise approach) between November 2008 and March 2010, 47 controls were selected based on these clinical characteristics at the time of the procedure: sex, presence of structural heart disease, and duration of continuous AF. The only exclusion criterion in the study and validation set was a prior AF ablation procedure. The study was approved by the institutional ethics committees, and all patients provided signed informed consent.

In addition to the following information, details regarding this study's methods are in the Online Appendix.

PROTOCOLS AND MAPPING. In the study population, only dispersion areas were ablated. For patients in sinus rhythm (SR) at the procedure's outset, AF was induced by rapid atrial pacing using the coronary sinus (CS) catheter (500 and 180 ms). If AF was not inducible, isoproterenol (baseline dose 2.4 mg/h, increased in 0.2-mg increments to obtain a sinus rate >100 beats/min) was infused. A reference AF cycle length (AFCL) value was calculated as the average of 2 consecutive measurements of 10 cycle lengths (CLs) either in the left atrial (LA) or right atrial (RA) appendages (Online Figure 1). The Online Appendix includes details on the validation set ablation procedure.

Medical; and has equity in and is a senior officer of Rhythm Solutions. Dr. Pisapia has received honoraria as a consultant for the STAR AF II trial from St. Jude Medical; and speaker fees from Medtronic. Dr. Kalifa is coinvestigator on a project sponsored by Medtronic; and owns shares of Volta Medical. All other authors have reported that they have no relationships relevant to the contents of this paper to disclose.

Manuscript received March 15, 2016; revised manuscript received September 29, 2016, accepted October 18, 2016.

FIGURE 1 Spatiotemporal Dispersion of Multipolar Electrograms

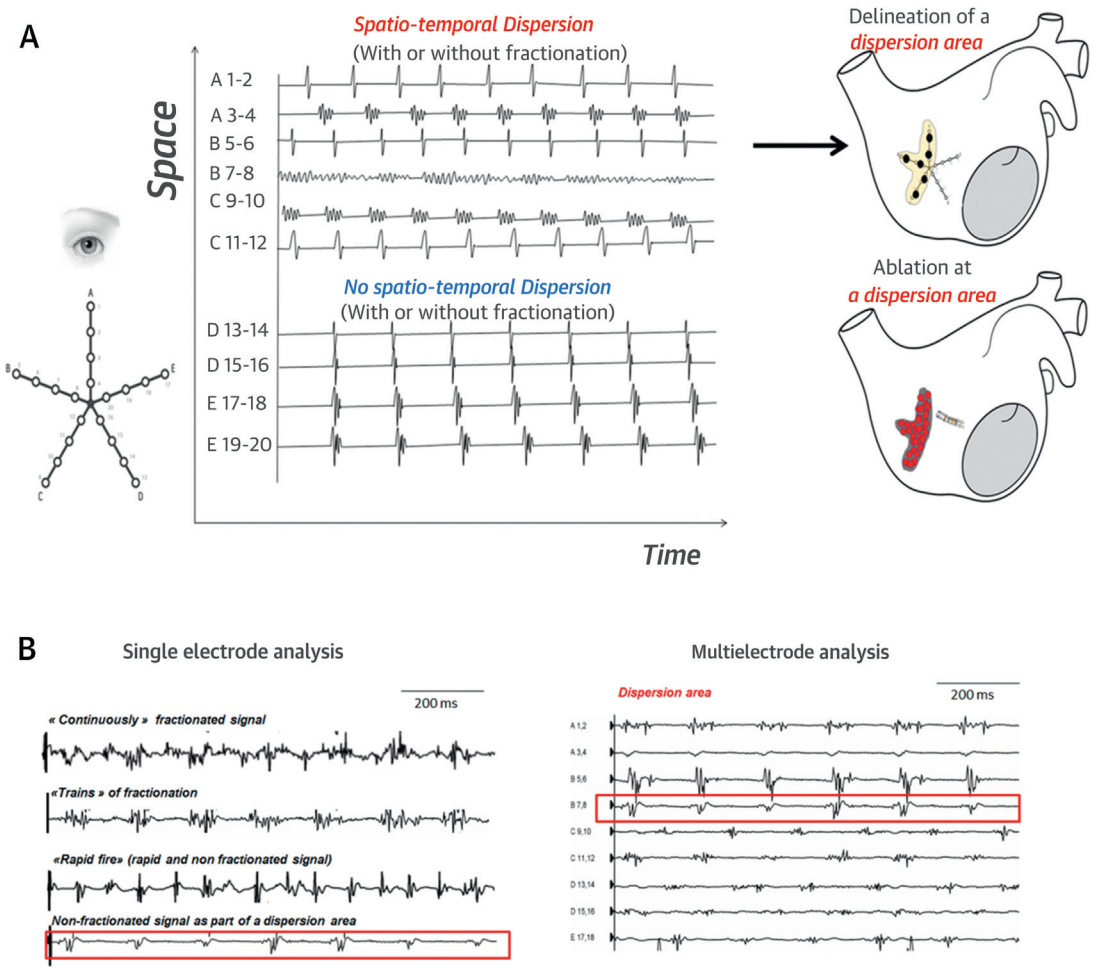

(A) Dispersion areas are defined and delineated via a mapping approach. **(B)** Single-bipole signals from dispersion regions were differentiated by fractionated or nonfractionated electrogram morphologies; nonfractionated (>120 ms) electrograms may be 1 or several of the electrograms within a dispersion region. Collectively, the bipolar electrograms span most of the atrial fibrillation (AF) cycle length recorded in the region.

Baseline mapping in both atria was performed during AF with the PentaRay multispline catheter (Biosense Webster, Diamond Bar, California) (Figure 1A) sequentially positioned in various regions of the RA and LA. At each location, the catheter was maintained in a stable position for a minimum of 2.5 s. The operator looked for dispersion areas (electrograms exhibiting both time and spatial dispersion). Where dispersion was found and/or the catheter was not stable for 2.5 s, acquisitions were repeated.

Dispersion areas were defined as clusters of electrograms, either fractionated or nonfractionated, that displayed interelectrode time and space dispersion at a minimum of 3 adjacent bipoles such that activation spread over all the AFCL (Figures 1A and 1B). At each bipole in a dispersion area, 1 or more of the following fractionated or nonfractionated electrogram morphologies were found (Figure 1B): 1) continuous, low-voltage fractionated electrograms ("continuously fractionated signal"); 2) bursts of fractionated electrograms ("trains of fractionation"); 3) fast nonfractionated electrograms (AFCL <120 ms; "rapid fires"); and 4) slow nonfractionated electrograms (AFCL >120 ms). Representative multipolar electrogram dispersion and nondispersion regions (Figure 2) illustrated that fractionated electrograms were found in both dispersion and nondispersion regions.

FIGURE 2 Examples of Spatiotemporal Dispersion

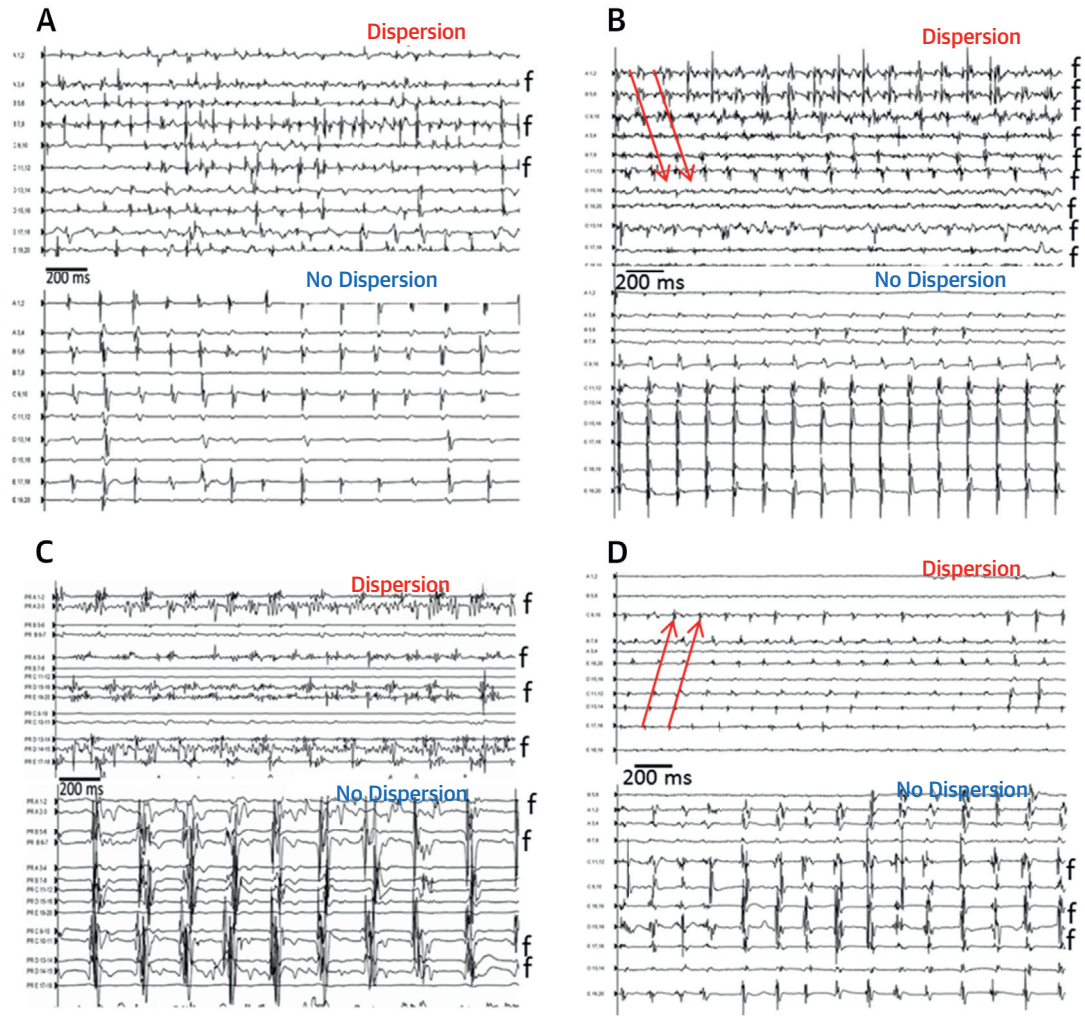

(A to D) These representative examples of multipolar electrograms were recorded in dispersion and nondispersion regions in 4 patients. In the dispersion regions, bipoles exhibiting continuously fractionated signal were common **(B and C)**. **f** indicates fractionated electrograms; **red arrows** indicate sequential activation of consecutive bipoles of multielectrode catheter spanning 100% of the atrial fibrillation cycle length.

ABLATION PROTOCOLS. We used a single transseptal sheath. Once initial biatrial mapping with the PentaRay catheter was obtained, there was no further analysis/evaluation performed either visually or quantitatively on electrograms recorded with the ablation catheter.

Radiofrequency (RF) energy was applied (10 to 45 W) at any atrial location including the PV antrum and the CS, whereas no ablation was performed inside the PVs. A contact force of 7 g was considered a minimum to deliver RF energy at any location. The power was adjusted to a range of 10 to 25 W when the ablation catheter was inside the CS, near a PV ostium, or on the posterior LA wall. The endpoint of ablation of areas of dispersion was AF termination defined as conversion to SR or a stable atrial tachycardia (AT) (15). Post-ablation ATs were mapped and ablated until conversion to SR. If AF did not terminate after ablation of the pre-selected dispersion area regions, a new multielectrode sequential map was performed (remapping). If 2 ablated areas were very close (<1 cm), they were connected by RF applications. Neither PV isolation nor linear ablation was performed.

After restoring SR by ablation, AF reinducibility was tested by rapid atrial pacing (500 to 180 ms) in the proximal and distal CS with the addition of

isoproterenol to induce AF when necessary. When ablation at dispersion regions led to rhythm regularization into AT before all dispersion regions had been ablated, the AT was mapped and ablated.

For patients in the validation set with paroxysmal AF, antral PVI was performed. For patients with persistent AF, ablation using the stepwise approach (16) was performed (details in the Online Appendix).

DISPERSION REGIONS. In 90 patients, the location of dispersion regions—as tagged on the 3-dimensional biatrial electroanatomic maps—was sorted according to biatrial segmentation as previously reported (15). The total surface area occupied by dispersion regions and the surface area of the ablated regions were measured from the electroanatomic maps in 43 patients. Biatrial surface was calculated after excluding areas pertaining to the mitral and tricuspid annuli, the vena cavas, and the PVs.

We evaluated inter- and intraobserver variability of the dispersion visual detection and the temporal stability of the spatial distribution of dispersion regions. (See the Online Appendix for methods.)

FOLLOW-UP. All patients were instructed to contact the study center if they experienced palpitations or any other symptoms suggestive of recurrent AF and to discontinue antiarrhythmic drug (AAD) therapy in the absence of symptoms after a 3-month blanking period. They also had follow-up visits and 24-h Holter monitors at 3, 6, 12, and 18 months. In a subgroup of 20 patients, the rhythm was monitored with 7-day Holter monitors ($n = 18$) or the memory functions of pacemakers and internal cardiac defibrillators ($n = 2$). Patients with recurrent AF or AT—defined as arrhythmia episodes >30 s after the blanking period—were offered a second ablation procedure. For redo procedures, the ablation protocol was similar to the one described for the study group.

STUDY ENDPOINTS. The primary short-term efficacy endpoint was AF termination. Secondary short-term efficacy endpoints were conversion to SR and post-ablation AF noninducibility. At the end of the 18-month follow-up period, our primary long-term efficacy endpoint was AF recurrence rate after a single procedure (with or without AAD therapy). Secondary long-term efficacy endpoints included: AF/AT recurrence rate after 1 procedure (with or without AAD therapy); AF/AT recurrence rate after 1 or more procedures (with or without AAD therapy); AF recurrence rate and AF/AT recurrence rate in the absence of AAD therapy (Online Appendix).

MECHANISTIC STUDY. We analyzed AT mechanisms and locations in a subset of 21 patients in whom post-ablation tachycardias occurred during the index procedure or during the follow-up.

We sought to compare the surface area occupied by CFAEs, classically used as ablation targets, with a dispersion region. We generated automatic fractionation maps ("auto-CFAEs") with the CARTO setting "SCI 30-40" (17) (CARTO, Biosense Webster), with 30 and 40 ms as lower and upper limits, respectively. In 40 regions (2 dispersion areas and 2 nondispersed regions in 10 patients), we calculated the auto-CFAEs surface area/dispersion surface area ratio and the auto-CFAEs surface area/nondispersion surface area ratio.

To examine the mechanisms of spatiotemporal dispersion in AF driver regions, we analyzed intracardiac electrograms in dispersion and nondispersion areas, which were the tagged and untagged regions, respectively. We also conducted numerical simulations and isolated ovine heart experiments to generate pseudomultipolar recordings in driver and bystander regions (Online Appendix).

STATISTICAL ANALYSIS. Categorical variables are expressed as n (%), and numerical variables as mean ± SD or median (interquartile range [IQR]). Categorical variables were compared using the chi-square test or Fisher exact test as appropriate. Continuous numerical data were compared using the Wilcoxon rank sum test or Brown-Mood median test as appropriate.

Survival analyses were performed to compare endpoints at the end of follow-up: Kaplan Meier estimates for AF rates after a single procedure; AF/AT rates after a single procedure; and AF/AT rates after ≥1 procedures (with or without AAD therapy) (Online Appendix). Kaplan-Meier survival curves were assessed and compared using log-rank tests. The time recorded was the time needed for the event of interest to occur (failure to achieve freedom from AF or freedom from AF and AT). The outcome was unknown in patients who did not reach the event before the end of follow-up (i.e., an 18-month follow-up), in patients lost to follow-up, and in patients who died during follow-up. In all such cases, time of follow-up was recorded and interpreted as censored data. Pairwise Cox hazards regression was used to compare survival of dispersion area subgroups (paroxysmal, persistent, and longstanding persistent). A 2-sided p value < 0.05 indicated statistical significance. All statistical analyses were performed using SAS version 9.1 (SAS Institute, Cary, North Carolina).

RESULTS

Between September 2013 and July 2014, 126 consecutive patients with AF were prospectively enrolled at

TABLE 1 Baseline Characteristics

	Study Population (n = 105)	Validation Set (n = 47)	p Value
Age, yrs	63 ± 11	58 ± 11	0.0046
Male	80 (76.2)	35 (74)	0.8191
AF type			
Paroxysmal	24 (22.8)	9 (19.2)	0.60
Nonparoxysmal	81 (77.2)	38 (80.8)	0.60
Maximum sustained AF duration, months	12.2 ± 20	19.4 ± 31.6	0.2457
Structural heart disease	38 (36)	14 (35)	0.4665
Hypertension	48 (45.7)	20 (42.5)	0.5217
Diabetes	13 (12.4)	5 (10.6)	0.5995
LA diameter, mm	45.6 ± 7.6	42.4 ± 12.4	0.09
LVEF, %	52 ± 11	54 ± 12	0.2082
Amiodarone before ablation, %	32	NA	
Spontaneous AF at the beginning of procedure (persistent and longstanding persistent AF only), n	65	NA	

Values are mean ± SD or n (%) unless otherwise indicated.
AF = atrial fibrillation; LA = left atrial/atrium; LVEF = left ventricular ejection fraction; NA = not applicable.

3 centers. Eighteen patients were excluded because of previous AF ablation, and 3 patients when an LA appendage thrombus was detected before ablation. In total, 105 patients were enrolled and compared to a validation set of 47 patients (Table 1).

MAPPING AND ANALYSIS. Before ablation, the RA and LA appendage reference CLs were 179 ms (IQR: 177 to 206 ms) and 182 ms (IQR: 164 to 203 ms), respectively. The mapping times and number of acquisition points per patient in the RA and LA were 7 min (IQR: 5 to 9 min) and 12 min (IQR: 10 to 15 min) and 491 (IQR: 325 to 704) points and 882 (IQR: 673 to 1,110) points, respectively.

Maps with representative dispersion areas in 3 patients with paroxysmal, persistent, and longstanding persistent AF illustrated that dispersion areas were formed by a variable number of electrograms (Figures 3A to 3C) and were patient- and AF type-dependent. There was an average of 5 ± 1.5 dispersion areas per patient, and each dispersion area spanned an average of 5 ± 2 cm^2 (Table 2). Dispersion areas covered a significantly larger surface area in patients with longstanding persistent AF than patients with paroxysmal or persistent AF. Dispersion area locations are in Table 3.

The visual analysis of the 4 operators was completely concordant in 94.3% of the analyzed electrograms (interobserver variability equal to 6.7%). The intraobserver variability of the visual analysis was 2 ± 2% (5%, 1.7%, 1.7%, and 0%, respectively for each operator).

We observed a high degree of temporal stability in the spatial distribution of dispersion regions, regardless of whether the repeat mapping was performed by the same or a distinct ablationist (detailed results are presented in the Online Appendix, Online Figure 2).

PROCEDURAL RESULTS. Ablation was performed in both the LA and RA in 51% of patients, with the procedural outcome seen in Figure 4 and Online Figure 3. In the remaining patients, ablation was only performed in the LA. AF terminated in 100 of 105 (95%) patients. In patients in "spontaneous" AF at the procedure outset, AF termination was obtained in 60 (92%). By comparison, AF termination was obtained in all patients in whom AF was pace-induced (n = 40; p = 0.15). Of note, there were 25 of 65 (33.8%) patients with spontaneous AF on AADs versus 12 of 40 (30.0%) with induced AF on AADs (p = 0.68). AF termination was obtained with 20 (IQR: 10 to 37) min of RF energy and 46 (IQR: 21 to 72) min after the first RF application either by conversion directly to SR (15%) or conversion to AT (85%) (Figure 4A). Overall, 77% of patients converted to SR via ablation.

Post-ablation AF inducibility was tested in 61 (58.6%) patients. Noninducibility of AF and AT was achieved in 44 (72%) of those tested. An average of 1.93 ± 1 ATs were ablated (Figure 4A). No major complications occurred. Three patients experienced minor groin bleeding. RF time to terminate AF was significantly longer in longstanding persistent AF versus both paroxysmal and persistent AF (p = 0.0004) (Figure 4B). The procedure time to terminate AF was significantly longer in longstanding persistent AF versus paroxysmal AF (p = 0.007) (Figure 4B). For total procedure and RF times, there was no difference between AF types (Figure 4C).

In the validation set, AF termination and SR conversion rates were significantly lower (Figure 4D). Also, the overall average procedure, RF energy, and fluoroscopy times were significantly longer in the control group: 230 ± 67 min versus 168 ± 42 min (p < 0.0001); 85 ± 35 min versus 49 ± 21 min (p = 0.0001); and 78 ± 25 min versus 15 ± 13 min (p < 0.0001), respectively (Figure 4E, Online Table 1). RF energy times for paroxysmal AF ablation were similar between the study population and the validation set (Online Table 1).

The area that was ablated represented 10 ± 5% of the overall biatrial area and 17 ± 10% of the LA area. Notably, the areas ablated in paroxysmal and persistent AF patients were comparable, but the area ablated in patients with longstanding persistent AF was significantly larger (Table 2).

LONG-TERM RESULTS. Ninety-six patients (91.4%) in the study population completed 18-month follow-up. Of the 9 (8.6%) who did not, 1 patient died 2 months before the end of follow-up (myocardial infarction),

FIGURE 3 Dispersion Maps

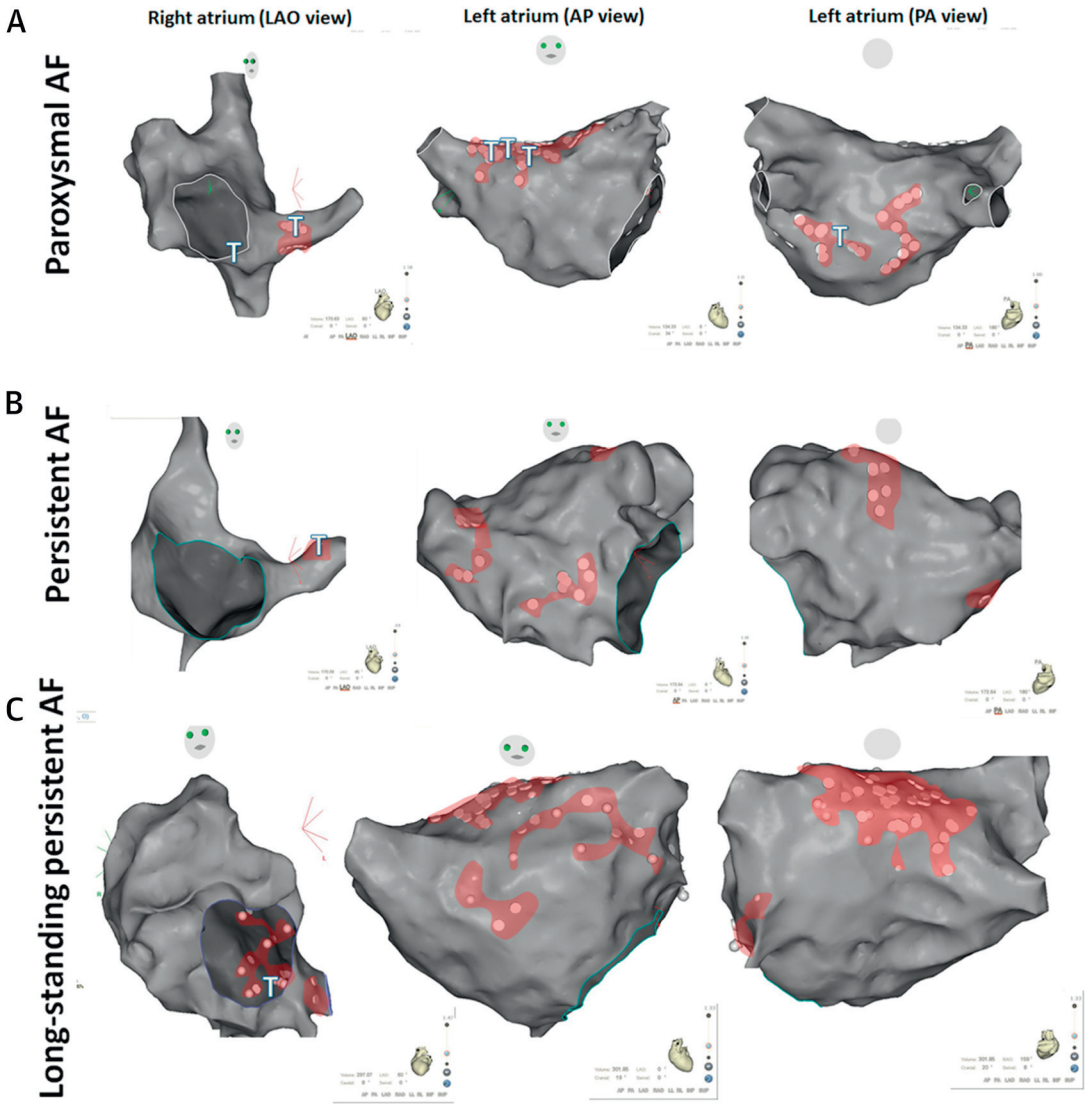

CARTO renderings show dispersion regions (in **red**) delineated by clusters of electrograms **(white dots)** in representative patients with **(A)** paroxysmal, **(B)** persistent, and **(C)** longstanding persistent AF. **T** indicates sites at which point ablation led to AF termination. AF = atrial fibrillation; AP = anteroposterior; LAO = left anterior oblique; PA = posteroanterior.

and 8 were lost to follow-up because of relocation. Their mean follow-up time was 10 ± 3 months. In the validation set, 3 patients dropped out during the blanking period (1 died of heart failure and 2 relocated). All other patients completed 18-month follow-up.

The single-procedural AF and AF/AT recurrence rates after 18 months were significantly lower in the study population compared with the validation set (11% vs. 58%; log-rank $p < 0.001$; and 45% vs. 64%; log-rank $p = 0.026$, respectively). AF-free (89% vs. 42%; log-rank $p < 0.001$) and AF/AT-free survival rates (55% vs. 36%; log-rank $p = 0.026$) also were significant (**Figure 5A**). The multiple-procedural arrhythmia recurrence rates were also lower in the study population at the end of the follow-up: 15% versus 41% (log-rank $p < 0.001$) as were AF/AT-free survival rates (85% vs. 59%; log-rank $p < 0.001$). (**Figure 5B**, Online Figures 4 and 5 show data from 7-day Holter-monitoring.) Importantly, there were comparable rates of patients using AADs in the study group versus the validation set (44% vs. 43%; $p = 0.9$).

TABLE 2 Surface Area

	All Patients (N = 43)	Paroxysmal (n = 15)	Persistent (n = 17)	LS Persistent (n = 11)	p Value
Dispersion areas					
Total dispersion area surface, cm^2					
Mean ± SD	22.5 ± 13.5	18 ± 10	17 ± 9	41 ± 12	<0.0001
Median (IQR)	19 (12.5-33)	17 (13-22)	15 (11-19)	40 (32-50)	
Mean dispersion area surface, cm^2					
Mean ± SD	5 ± 2	5 ± 2	4 ± 1.5	6 ± 2	0.0025
Median (IQR)	4.5 (3-6)	4.5 (3.4-6.0)	3.2 (2.9-5.6)	6.0 (4.9-8.2)	
Number of dispersion areas					
Mean ± SD	5 ± 1.5	4 ± 1.7	5 ± 1.2	6 ± 1	0.02
Median (IQR)	5 (4-6)	4 (3-5)	5 (4-5)	6 (5-7)	
Ablation in the RA					
RA ablated surface, cm^2					
Mean ± SD	6 ± 5	4 ± 5	5 ± 3	9 ± 7	0.03
Median (IQR)	4.5 (2-7)	3 (0-4)	5 (2-6)	7 (4-15)	
RA total surface, cm^2					
Mean ± SD	154 ± 58	138.3 ± 71.0	138.9 ± 36.5	196.5 ± 50.2	0.003
Median (IQR)	150 (122-184)	129 (121-186)	135 (117-169)	186 (167-220)	
Percent of RA ablated surface					
Mean ± SD	4 ± 2.5	3.8 ± 3	4.2 ± 3	4.0 ± 2.5	0.90
Ablation in the LA					
LA ablated surface, cm^2					
Mean ± SD	25.5 ± 15.7	20.5 ± 10.5	16.5 ± 6	46 ± 13.5	<0.0001
Median (IQR)	20.6 (15-35.5)	19 (14-27)	17 (11-21)	40 (36-56)	
LA total surface, cm^2					
Mean ± SD	157 ± 47	139 ± 44	167 ± 53	165.5 ± 35	0.18
Median (IQR)	156 (135-171)	153 (114-164)	156 (135-172)	165 (152-175)	
Percent of LA ablated surface					
Mean ± SD	17 ± 10	15.8 ± 8.8	10.1 ± 4.0	29 ± 9.7	<0.0001
Ablation in both atria					
Biatrial total surface, cm^2					
Mean ± SD	302 ± 85	266 ± 97.5	296 ± 53	361 ± 82.5	0.06
Median (IQR)	312 (257-350)	288 (207-331)	293 (273-322)	340 (320-398)	
Bi-atrial total ablated surface, cm^2					
Mean ± SD	31 ± 19	25 ± 12	21 ± 7.0	55 ± 17.5	<0.0001
Median (IQR)	24.5 (18-39.5)	21 (17-39)	20 (16-23)	50 (42-74)	
Percent of biatrial ablated surface, cm^2					
Mean ± SD	10 ± 5	10 ± 4	7.5 ± 2.5	15 ± 4	0.0005

IQR = interquartile range; LA = left atrial/atrium; LS = longstanding; RA = right atrial/atrium.

TABLE 3 Distribution of Dispersion Areas

Regions	Dispersion Areas* (% of Patients)
Left pulmonary veins and left appendage	79
Right pulmonary veins and posterior interatrial groove	78
Inferior and posterior LA	73
Upper half of RA and appendage	42
Lower half of RA	31
Anterior LA and roof	77
Anterior interatrial groove	77

*For each atrial subregion, the percentage indicates the proportion of patients in whom at least 1 dispersion area was counted.

Abbreviations as in Table 2.

After 1 procedure, there were no differences in AF recurrence or AF/AT recurrence rates between the paroxysmal, persistent, and longstanding persistent groups: respectively, 21%, 8%, and 10% (log-rank p = 0.24) and 29%, 53%, and 43% (log-rank p = 0.15). After 1.4 ± 0.5 procedures per patient, there also were no differences in AF/AT recurrence rates between the paroxysmal, persistent, and longstanding persistent groups, respectively: 17%, 16%, and 13%; log-rank p = 0.9. Redo procedures were performed for organized ATs in 75.6% of patients. Redo procedures were significantly shorter in duration than the index procedures and required less RF and fluoroscopy times (Table 4). Except for 1 pericardial effusion, no

FIGURE 4 Procedural Outcomes

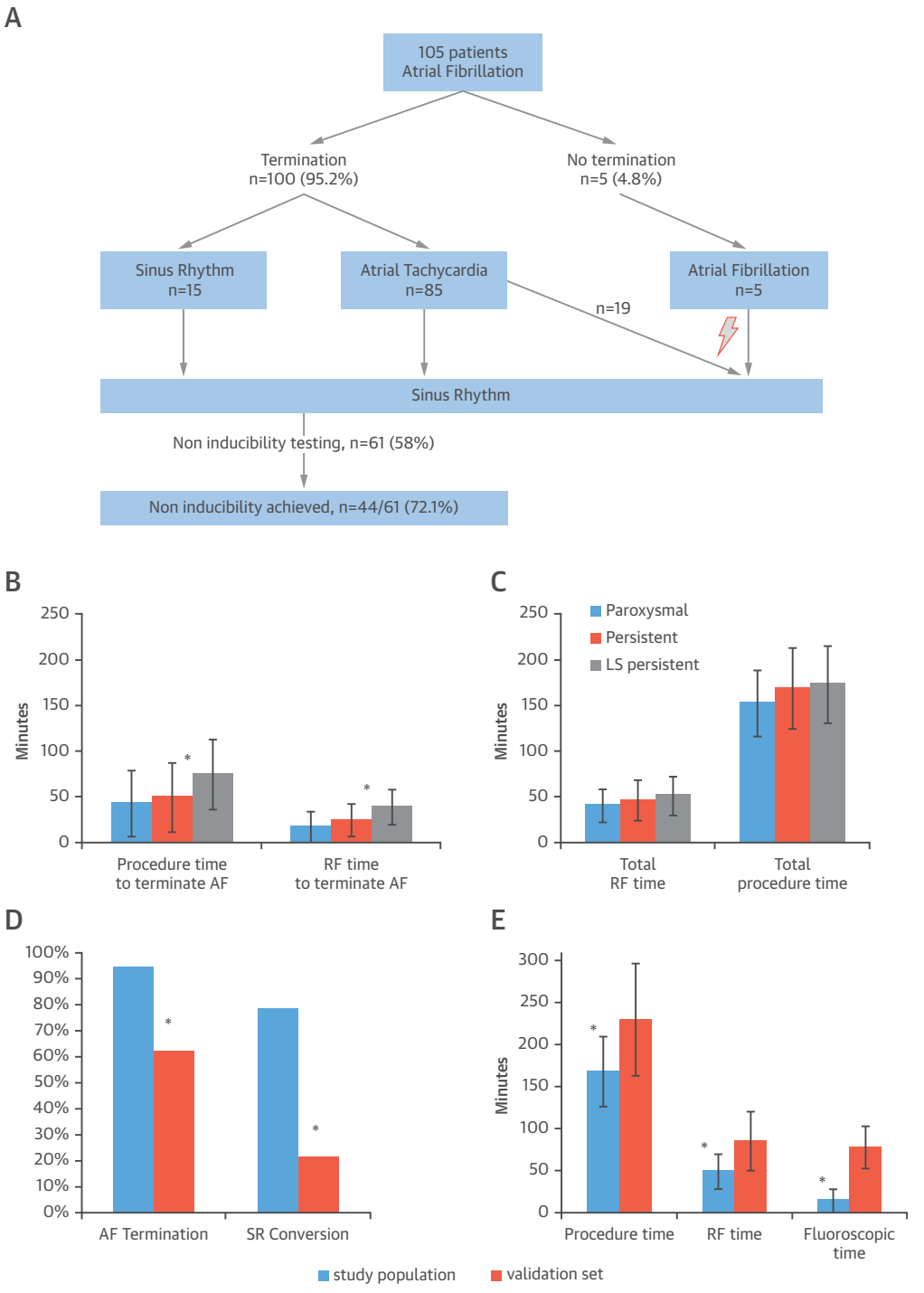

(A) This study flowchart shows outcomes per procedure. The thunderbolt represents electrical cardioversion at the end of the procedure. Although both **(B)** procedure and radiofrequency (RF) time to terminate atrial fibrillation (AF) were significantly higher in longstanding (LS) persistent AF compared with persistent AF, there were **(C)** no significant differences among types in total procedure or RF times between all AF types ($p > 0.05$). In comparing the study and validation populations, **(D)** the former achieved significantly higher rates of AF termination and sinus rhythm (SR) conversion by ablation at lower **(E)** procedure, RF, and fluoroscopic times. *$p < 0.01$.

FIGURE 5 18-Month Outcome

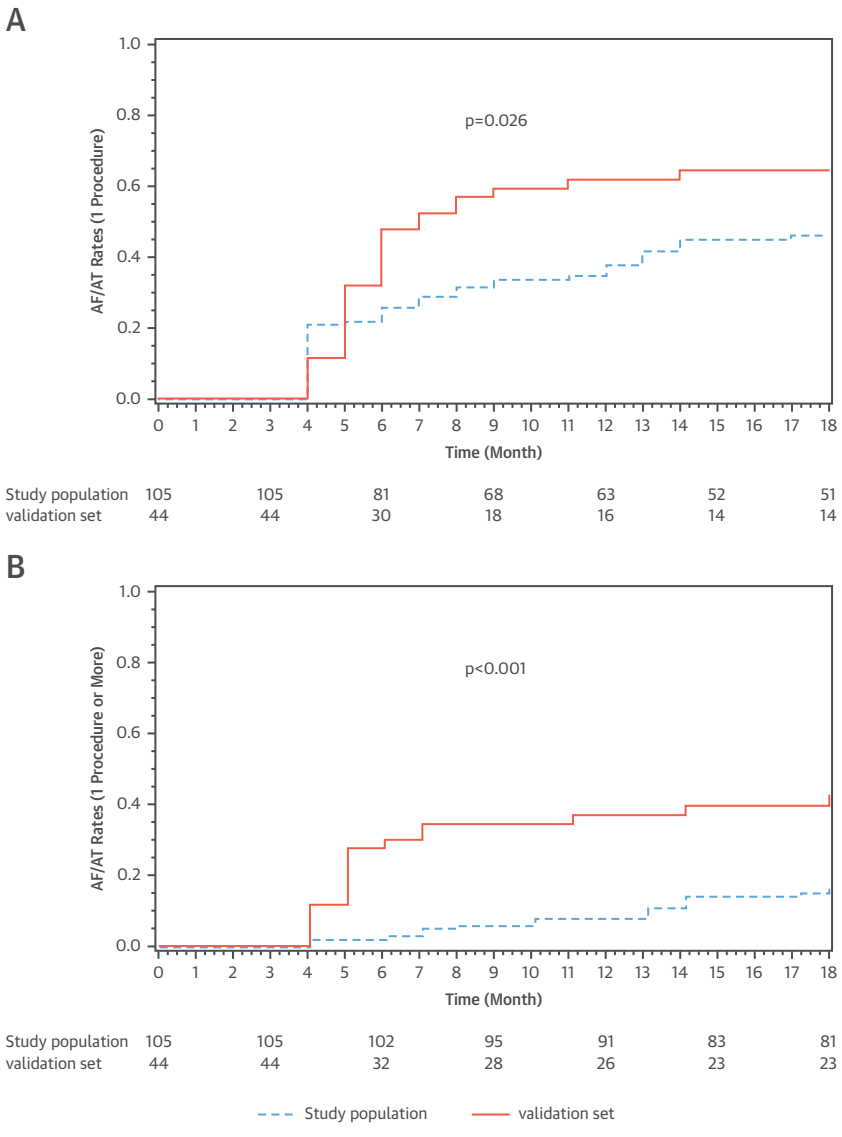

Kaplan-Meier curves show atrial fibrillation (AF)/atrial tachycardia (AT) recurrence rates after **(A)** a single procedure and after **(B)** multiple procedures in the study population and the validation set.

major complications were noted after the redo procedures.

We then compared key patient and procedural characteristics between patients who were "spontaneously" in AF at the beginning of the procedure (no pacing maneuver) versus those in whom AF had been pace-induced. For pace-induced and "spontaneous" AF patients, respectively, LA volumes were 143 ± 31 ml versus 181 ± 46 ml ($p < 0.0001$); RF time to terminate AF 19.8 ± 16.2 min versus 29.4 ± 20.4 min ($p = 0.02$); total RF times 43 ± 19.7 min versus 52.3 ± 21.5 min ($p = 0.01$); and rates of AF termination, 100% and 92% ($p = 0.15$). However, after 18-months follow-up and an average of 1.4 procedures in both subgroups, there was a similar rate of AF/AT recurrence between "spontaneous" AF and pace-induced AF (14% vs. 18%, respectively; log-rank $p = 0.44$). We observed no statistical difference in outcomes at the end of the follow-up between patients on and off AADs: single-procedure AF recurrence rate was 13% for those on versus 10% for those off drugs (log-rank $p = 0.62$); the single-procedure

TABLE 4 Per-Procedural Outcome (Index and Redo Procedures)

	Rhythm	Procedure Time (min)	RF Time (min)	Fluoroscopic Time (min)	Sinus Rhythm Conversion	Noninducibility Tested and Obtained
Ablation procedure # 1 (n = 105)	AF = 100%	168 ± 42	49 ± 21	15 ± 13	77%	42%
Ablation procedure # 2 (n = 38)	AF = 24% (AT =76%)	125 ± 43*	27 ± 21*	10 ± 10*	85%	64%
Ablation procedure # 3 (n = 3)	AF = 33% (AT=67%)	109 ± 8*	17.5 ± 10*	7 ± 4*	100%	100%

Values are mean ± SD or %. *$p < 0.005$.

AF/AT recurrence rate was 46% for those on versus 44% for those off drugs (log-rank p = 0.71); and the AF/AT recurrence rates after 1 or more procedures was 15% in patients on or off drugs (log-rank p = 1.00).

MECHANISTIC STUDY. In 21 patients, we counted 44 distinct ATs (2.2 ± 1.3 AT per patient): 22 were macro-re-entries (peritricuspid, perimitral, or LA roof flutters) and 22 were localized AT (focal or micro-re-entries). Of these 44 ATs, only 5 (11.4%) originated from dispersion regions that had just been ablated, whereas 39 (88.6%) were either macro-re-entries or localized ATs arising from locations not previously ablated. Importantly, 17 of 22 localized ATs arose from dispersion regions not previously ablated (Online Figure 6).

We analyzed long-term AT recurrences after the index AF ablation procedure. We focused our analysis on determining whether the AT that occurred arose from the dispersion regions that were targeted during the index procedure (dispersion-index regions) or from nondispersion regions (nondispersion-index regions), which were not ablated. During follow-up, 11 AT ablation procedures were conducted. Of 18 distinct recurrent ATs, 11 (61%) originated from nondispersion-index regions as follows: 6 macro-re-entries previously ablated at nondispersion regions such as the mitral isthmus or the roof, relapsed presumably because of conduction recovery of ablation lines; 4 macro-re-entries not present during the index case; and 1 focal tachycardia from a nondispersion-index region. Additionally, 3 (16.6%) originated from within a dispersion-index region and 4 (22%) were found in close vicinity of a dispersion-index region (<1 cm).

The ratios of surface area of CFAEs automatically detected to the surface area of dispersion regions and to the surface area of regions not displaying dispersion were 72 ± 25% and 27 ± 15%, respectively (**Figure 6A**, Online Figure 7).

Dispersion area abnormal electrograms exhibited a higher occurrence of single-bipole fractionated continuous signals (**Figure 6B**), a reduced voltage (**Figure 6C**), a significantly shorter CL (**Figure 6D**), and a dispersion duration that spanned most of the AFCL (**Figures 6E and 6F**). Additionally, a mean of 8.1 ± 3.5 rotations per 2.5 s occurred in dispersion areas (**Figure 6G**).

Figure 7 depicts simulated pseudo-multipolar electrograms obtained after positioning a virtual PentaRay either at the center or at periphery of the driver (here a rotor) (**Figures 7A to 7C**, Online Video 1). In comparing **Figure 7A and 7B**, striking differences in the features of the virtual PentaRay electrograms can be seen. When the virtual catheter hovered over the center of the driver, virtual bipolar electrograms exhibited a fast frequency of excitation. Also, the time distribution of the electrograms was such that either branch of the PentaRay was activated in asynchrony with the other branches. Consequently, the virtual electrogram time-series spanned most of the AFCL. The overall visual impression was one of successive electrode-to-electrode and branch-to-branch activations. At the driver periphery, the frequency of activation was reduced and impulses were nonrotational or planar-like. As a result, either branch of the PentaRay was activated in relative synchrony with the other branches (**Figure 7B**). The visual impression was one of successive beats separated by quiescence.

Figure 7C shows an AF driver initiated in a pseudofibrotic substrate. In this setting, driver impulses propagated within a highly heterogeneous substrate. The virtual PentaRay then generated unique multipolar pseudoelectrogram features. Throughout the 2-dimensional sheet, multiple regions contributed to a slowing down of the rotational impulse. Although there was no impulse block, the driver's wavefront experienced markedly slow and heterogeneous conduction. This resulted in beat-to-beat changes in wave directionality. Such disturbances translated into lengthened and fractionated depolarization pseudoelectrograms (**Figure 7C**), reminiscent of the features of dispersion areas in patients. Here, the numerical and experimental data predicted that such drivers should yield electrograms with significantly greater temporal and spatial dispersion than drivers spinning within relatively homogeneous media.

FIGURE 6 Signal Analysis

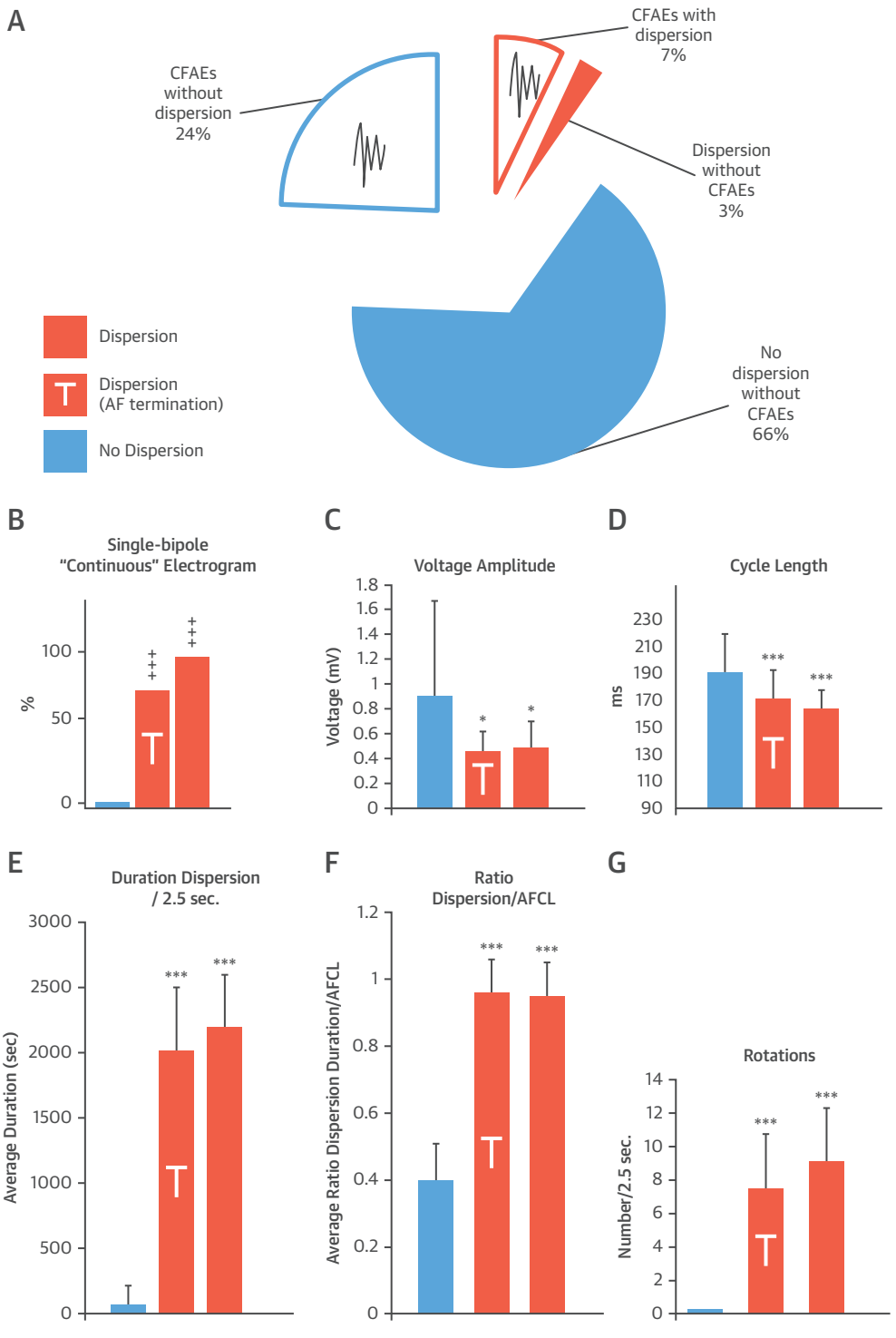

(A) The surface area of complex fractionated atrial electrograms (CFAEs) varied in dispersion and nondispersion regions. An off-line analysis of electrograms from dispersion areas and from nondispersed regions showed significant differences in regard to **(B)** single-bipole "continuous" electrogram; **(C)** voltage amplitude; **(D)** cycle length (CL); **(E)** duration of spatiotemporal dispersion per 2.5 s; **(F)** ratio of spatiotemporal dispersion per atrial fibrillation (AF) CL (AFCL); and **(G)** rotations. Mean ± SE; *$p < 0.05$; ***$p < 0.01$; +++$p < 0.05$ (Kruskal-Wallis); $n = 20$ patients; $n = 68$ and $n = 35$ dispersion areas and nondispersed regions, respectively. **T** indicates the dispersion area at which AF terminated.

FIGURE 7 **Numerical Simulations**

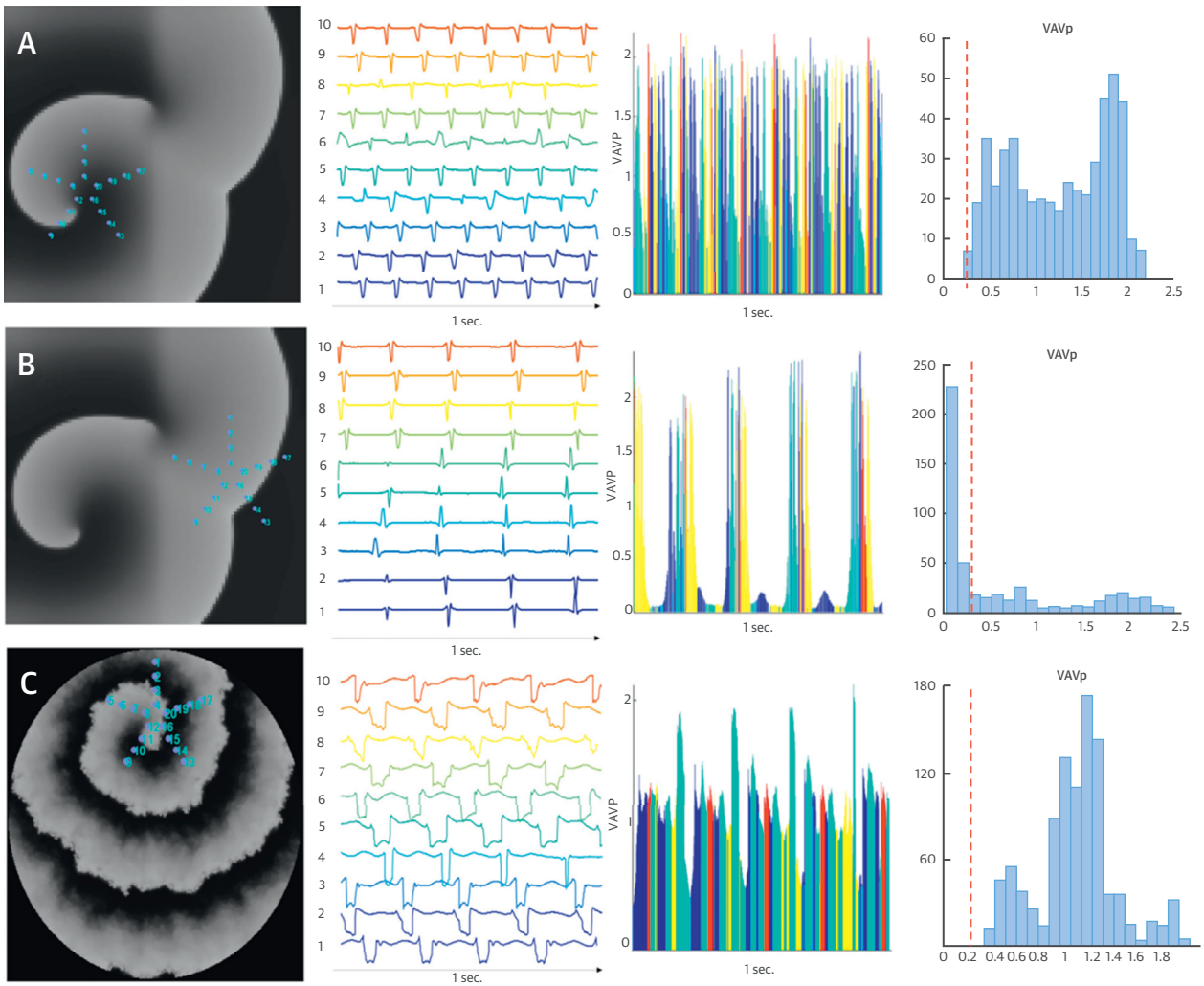

In a human atrial model with homogeneous substrate, the virtual PentaRay is positioned **(A)** at the center of the driver, and the aspect of the pseudomultipolar electrograms is one of spatiotemporal dispersion, reminiscent of patients' dispersion areas, and **(B)** at the periphery of the driver in a region activated at a slow frequency of excitation (Online Video 1). **(C)** In the interstitial fibrosis condition (myocyte/myofibroblast ratio: 0.5), the pseudomultipolar electrograms exhibit a large spatiotemporal dispersion. The VAVmax among the 10 pseudobipoles of the virtual PentaRay was collected at each time point to form a new time series VAVp. Histograms of the distribution of VAVp values are presented in bins of 0.1 mV. Low VAVp values are underrepresented in the driver regions, whereas they are predominant in bystander regions **(red dashed line)**. VAV = voltage absolute value; VAVp = Time series of maximal voltage absolute values at any of the bipoles.

OPTICAL MAPPING. **Figures 8A and 8B** included pseudomultipolar electrograms generated from optical movies during AF induced in an isolated LA scar (Online Appendix). The PentaRay-like single-pixel time series was obtained in the region of the LA myocardial infarct border zone where a driver was anchored after initiation by burst pacing (Online Video 2). For comparison, we presented PentaRay-like single-pixel time series obtained at the RA where nonrotational and planar-like waves propagated (Online Video 2). Similar to the differences seen in the simulations, fractionated multipolar pseudoelectrograms exhibited a high degree of spatiotemporal dispersion when recorded in the vicinity of a driver (**Figure 8B**, right). In the RA bystander region, however, waves were planar-like and pseudoelectrograms were nearly simultaneous (**Figure 8B**, left).

These aspects evoked the dispersion areas and nontagged multipolar electrogram aspects recorded in patients. Furthermore, the time series of maximal voltage absolute values at any of the bipoles shown in the right panels of **Figures 7 and 8** illustrated that the

FIGURE 8 Optical Mapping

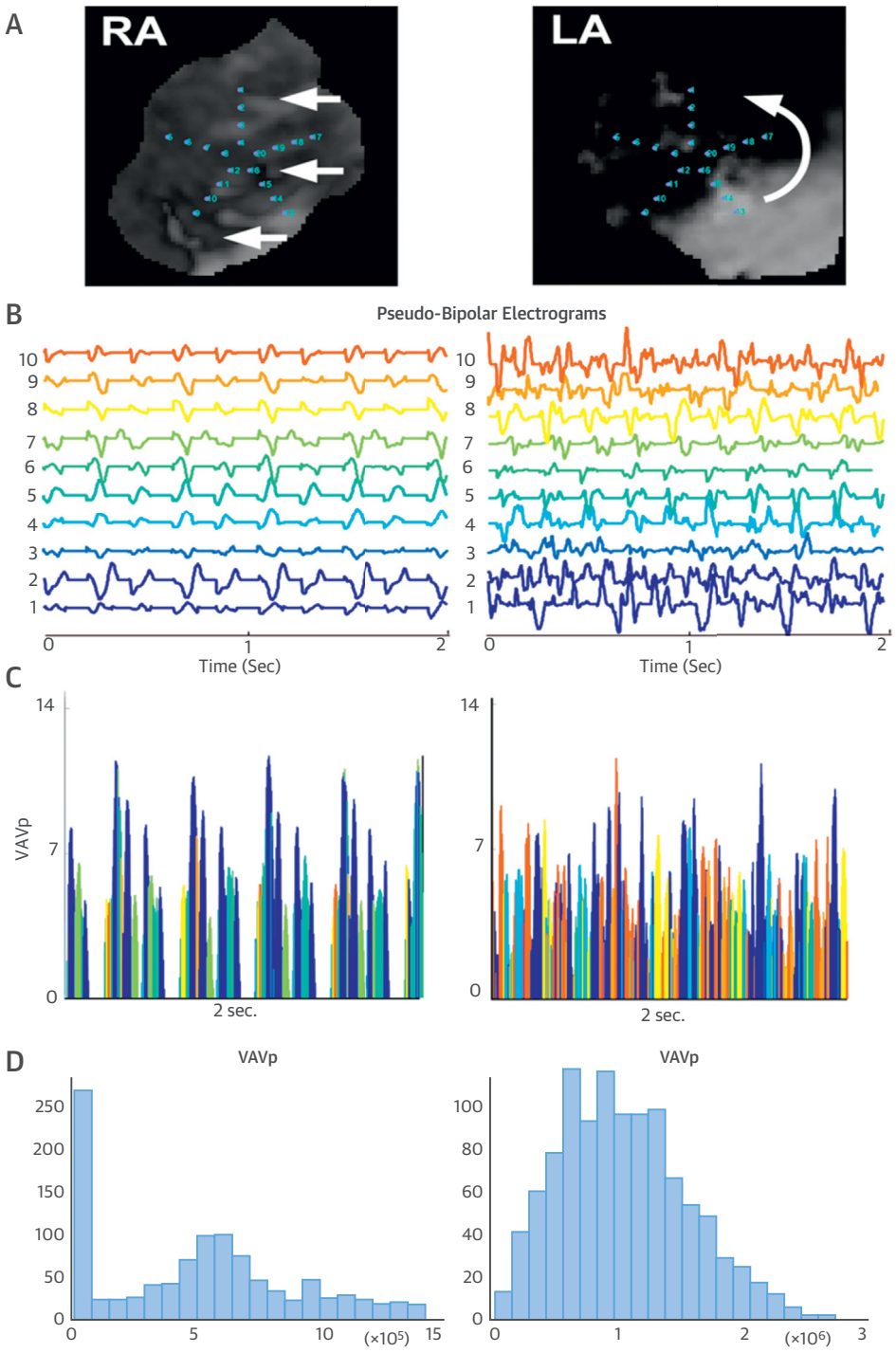

In this pseudomultipolar single-pixel time series in a left atrial (LA) scar, the right atrium (RA) displays planar-like waves that yield little spatiotemporal dispersion (Online Video 2); in terms of the LA driver, however, aspects reminiscent of patients' spatiotemporal dispersion are seen in **(A)** optical movie snapshots during AF; **(B)** pseudobipolar electrograms; **(C)** VAVp time series; and **(D)** histograms of the distribution of VAVp values. Low VAVp values are underrepresented in the LA driver region, whereas they are predominant in the RA bystander region.
VAVp = Time series of maximal voltage absolute values at any of the bipoles.

time of electrical quiescence of pseudo-multipolar electrograms obtained in the vicinity of a driver—that is, low <0.2 mV voltage absolute values at any of the bipoles—was drastically reduced in comparison with the time of electrical quiescence of pseudomultipolar electrograms from bystander regions. Collectively, our simulations and optical mapping studies suggested that dispersion areas may be regarded as electrogram footprints of active electrical sources of AF propagating in a heterogeneous atrial muscle.

DISCUSSION

Our main findings are as follows: 1) spatiotemporal dispersion of electrograms represented an electrical footprint of waves emanating from rapid fibrillatory drivers and propagating within a heterogeneous atrial muscle; and 2) the clustering of intracardiac electrograms exhibiting spatiotemporal dispersion may guide a wholly patient-tailored ablation of all types of AF.

This pilot study's results demonstrated that electrogram dispersion detected by direct visualization of electrograms recorded simultaneously with a splined, multielectrode catheter is a marker of AF drivers. We recorded regions exhibiting spatiotemporal electrogram dispersion and targeted such regions in the absence of PVI or any other anatomy-based ablation. With 44% of patients on AADs, preliminary results showed that our approach allowed for efficacious, nonextensive, and wholly patient-tailored ablation of all AF types. Application of 20 min of RF energy resulted in a 95% rate of AF termination and 89% of patients free from AF after a single procedure, which continued during 18 months of follow-up. The AF/AT-free survival rate was 55% after 1 procedure and 85% after ~1.4 procedures per patient.

This study offers insight into why CFAEs might represent worthy ablation targets in some hands (6–8), but not in others (1–5). Successful outcomes after ablating CFAEs might be explained by the fact that fractionated electrograms represent a majority of the surface area in driver regions (**Figure 6A**), which exhibit spatial and temporal dispersion. Conversely, fractionated electrograms can also be found in bystander regions that do not exhibit dispersion (**Figures 2C and 6A**, Online Figure 7). We showed that CFAEs located in nondispersion regions represented most of the CFAE surface area. About 30% of the surface area in dispersion regions were sites of nonfractionated electrograms (**Figure 6A**). Altogether, we presented evidence that dispersion ablation might overlap with conventional CFAE ablation when CFAEs are spatially clustered. Also, our numerical and experimental data strongly suggested that dispersion regions correspond to driver regions, which may be identified either on the endocardial or epicardial sides of the atrial wall. Future works implementing advanced mapping simultaneously to multipolar electrode recordings are needed to examine the degree of overlap between driver and dispersion regions.

Our contribution aligns well with Narayan et al. (14) and Jadidi et al. (18) in that they suggested that patient-tailored, mechanism-based ablation may yield valuable results. We envision such studies, including our own, as building blocks of a collaborative effort that may lead to an efficacious patient-tailored ablation approach. In the study by Narayan et al. (14) the ablation time for reaching the short-term endpoint of AF termination or ≥10% AF slowing was 31.8 min (IQR: 22.1 to 71.5 min) and 18.5 min (IQR: 7.9 to 24.5 min) in the focal impulse and rotor modulation-blinded and the focal impulse and rotor modulation groups, respectively. After PVI, ablation times increased to 52.1 ± 17.8 min and 57.8 ± 22.8 min, respectively. Jadidi et al. (18) showed that PVI as the initial ablation approach was achieved after a mean of 28 ± 11 min. Among patients in whom PVI did not terminate AF, selective atrial ablation at low-voltage, dispersion-like regions terminated persistent AF after 11 ± 9 min of RF. Ablation of the remaining ATs required an additional 12 ± 9 min, producing an RF time of 23 ± 11 min in addition to PVI, resulting in a grand total of 44 ± 19 min of RF (18). The main difference, however, with the present work was the percentage of the overall ablation time dedicated to patient-tailored ablation. This represented about one-third the overall ablation time reported by Narayan et al. (14) and one-half that reported by Jadidi et al. (18). Therefore, we feel that the most novel aspect of our approach was that it represented an approach that is entirely patient-tailored (**Central Illustration**).

The comparison with a validation set provided further evidence that dispersion ablation was comparable to a more conventional ablation approach (**Figures 4 and 5**, Online Table 1). Finally, after dispersion ablation, the majority (75.6%) of recurrences were organized AT and not AF. ATs were simpler to ablate as demonstrated by the reduced procedure time and the higher SR conversion rate during redo ablation (**Table 4**). We believe such a high proportion of AT/AF recurrences might be the basis for our highly satisfactory long-term outcomes: 85% of patients free from any arrhythmia after ~1.4 procedures per patient in a population with 77% of persistent and longstanding AF.

We conducted numerical simulations and experiments to examine the mechanisms by which regions harboring spatiotemporal dispersion of electrograms

CENTRAL ILLUSTRATION **Wholly Patient-Tailored Ablation Approach Guided by Spatiotemporal Dispersion of Electrograms**

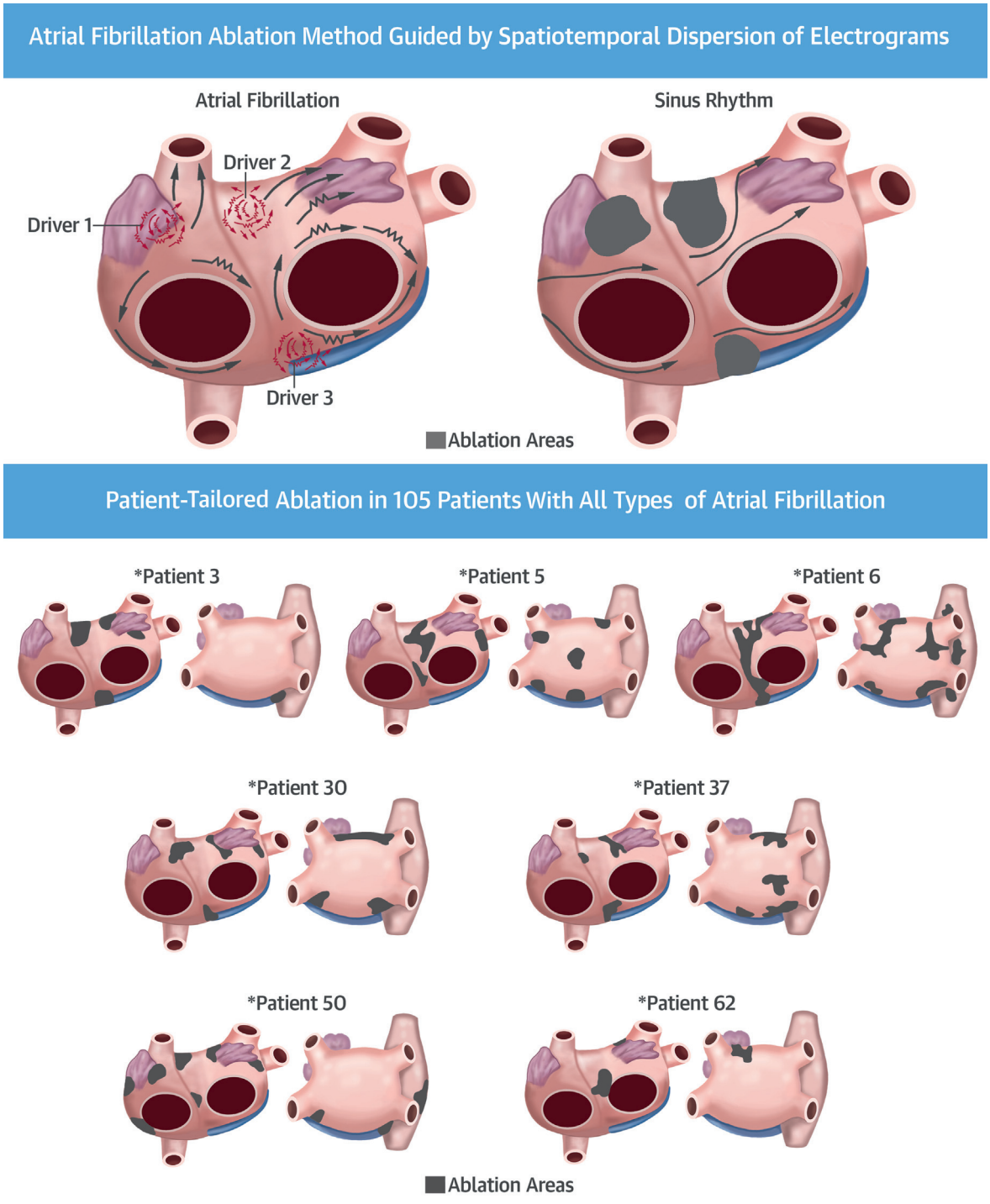

Seitz, J. et al. J Am Coll Cardiol. 2017;69(3):303–21.

Continued on the next page

are key to AF perpetuation. Both our experiments and numerical simulations showed that pseudomultipolar electrograms exhibiting dispersion were uniquely recorded in the vicinity of drivers (**Figures 7 and 8**). Such results illustrated that the simultaneous presence of time and spatial dispersion of abnormal electrograms represents regions where the wavefront shape is highly curved and where impulse propagation of waves emanating from drivers is impaired. This also corroborates previous findings that continuously fractionated electrograms, which could be dispersed electrograms, have been recorded in rotor regions (15) or in regions critical to AF maintenance (6–8). Importantly, our results demonstrated that dispersion of multipolar electrograms highly depends on both the source's frequency of activation and its underlying atrial substrate (**Figures 7 and 8**). We previously reported that beat-to-beat changes in wavefront directionality and impulse velocity produced fractionation in the immediate vicinity of a rotor at the boundary of the maximal dominant frequency domain (19). This was expected because several studies had emphasized that electrogram fractionation is highly frequency-dependent (11,19–21). In particular, Spach et al. (20) presented that electrogram fractionation that occurs during transversal impulse propagation might also manifest in the longitudinal direction at shorter CLs (frequency-dependent space dispersion). Here, our results corroborated these findings in showing that spatiotemporal dispersion of multipolar electrograms is frequency dependent. Therefore, our results also validated the studies that indicated that high dominant frequency may be used as a surrogate for AF source localization (22–24).

The fact that post-ablation ATs predominantly arise from nonablated dispersion regions suggests the unmasking of AT drivers after some degree of substrate modification. Although a plausible scenario, it is unclear how ablation may prevent fibrillatory conduction of waves emanating from the (subsequent) AT drivers while, at the same time, reducing the overall frequency of activation. This would suggest that a single ablation application could produce effect on an AT driver as well as on distant waves emanating from it. A possible alternative scenario: post-ablation ATs arising from nonablated dispersion regions preexist but as secondary or co-primary drivers, and once 1 or more drivers have been ablated, the arrhythmic activity may only be maintained by slower drivers. These may only rise to dominance once their faster counterpart, located in a distinct dispersion region, has been ablated.

We further demonstrated that interstitial fibrosis was key to the observation of spatiotemporal dispersion of electrograms during AF. Previously, we and others had reported that fractionated electrograms may be recorded in regards of rotors propagating within a fibrotic atrium (24,25). Here, we showed that a driver initiated within a fibrotic atrium (**Figure 7C**) yielded a significantly larger temporal and spatial electrogram dispersion than the one produced by a driver propagating within a more homogeneous medium (**Figure 7B**). As we have previously shown (24), the presence of fibrotic, millimeter-sized obstacles (1 to 7 mm^2) is sufficient to anchor re-entries characterized by a CL that depends on the obstacle size. Therefore, in the context of extensive fibrosis, the term *rotor*, which might be understood as an "entirely functional" re-entry, may be interchangeable with terms such as *micro-re-entry* or re-entry that also are AF drivers. Overall, these results agree with recent atrial structural imaging reports, which have presented that the atria of patients undergoing AF are highly fibrotic, and that electrogram fractionation occurs in regions of patchy fibrosis (26–28).

STUDY LIMITATIONS. The nonrandomized design of this pilot study limited our conclusions in comparing techniques. An evaluation of dispersion area ablation in a larger patient population using a randomized study design is warranted. Also, in patients in SR at the outset of the procedure and in whom AF is initiated by pacing maneuvers, the assumption should be that RF ablation may lead to a serendipitous termination. In general, procedural endpoints such as AF

CENTRAL ILLUSTRATION Continued

Upper panel: Left: Before ablation, 3 drivers **(red arrows)** as well as bystander regions **(gray arrows)** are schematized. The arrow length is proportional to local electrogram cycle length. Fractionated electrograms **(red sinusoïdal arrows)** are most often located in driver regions but can be observed in nondispersion, nondriver regions **(red and gray sinusoïdal arrows). Right:** After wholly patient-tailored ablation of the 3 driver regions represented in the **left panel**, AF termination ensued. **Lower panel:** Schematic depiction in 7 of 105 patients from the study with all types of AF (paroxysmal, persistent, and long-standing persistent) of the regions harboring spatiotemporal dispersion, which were subsequently ablated. The location and extent of spatiotemporal dispersion regions were unique to each patient. In this study, AF was terminated in 95% of the patients, 85% maintained arrhythmia free-survival at 18 months following ~1.4 ablation procedure/patient and had experienced shorter radiofrequency and procedure times in comparison to a more conventional ablation approach.

termination, SR conversion, or AF noninducibility need to be interpreted with caution. Besides, their value as procedural predictors of long-term outcome will need to be rigorously investigated.

We did not check whether PVs were isolated. Therefore, we cannot state that some of the PVs were not unintentionally isolated. In 13 additional patients, in whom we only performed dispersion ablation, only 2 of 52 PVs were isolated unintentionally.

The computer simulations were performed in a 2-dimensional model; a more realistic 3-dimensional model of AF and fibrosis would yield more realistic electrograms. Finally, to avoid prolonged procedures and comply with institutional requirements, we made the collegial decision to withhold inducibility maneuvers after 2 h.

CONCLUSIONS

We presented the first demonstration that the clustering of intracardiac electrograms exhibiting spatiotemporal dispersion allows for a wholly patient-tailored ablation of all types of AF.

ACKNOWLEDGMENTS The authors thank their colleagues for their scientific input, in particular Drs. Fred Morady, Hakan Oral, José Jalife, Alexandre Maluski, Eloi Marijon, and Julien Mancini. The authors also thank Fanny Desmettre, Julia Legrand, Alexandrine Lozupone, Camille Metzdorff, Joseph Ajoury, Alexandre Masse, and Kamila Djouadi for their technical assistance. Special thanks to Donovan C. Jr. for his drawings and his support.

REPRINT REQUESTS AND CORRESPONDENCE: Dr. Julien Seitz, Hôpital Saint Joseph, Unité de Rythmologie Interventionnelle, Service de Cardiologie, 26 Boulevard de Louvain, 13008 Marseille, France. E-mail: jseitz@hopital-saint-joseph.fr.

PERSPECTIVES

COMPETENCY IN PATIENT CARE AND PROCEDURAL SKILLS: Spatiotemporal dispersion of multipolar electrograms recorded during catheter ablation is a signature of electrical drivers of atrial fibrillation in the left and right atria. Ablation at these locations often eliminates AF.

TRANSLATIONAL OUTLOOK: Additional research is needed to assess the long-term outcomes of ablation procedures guided by automated software that identities spatiotemporal electrogram dispersion in patients with various patterns and durations of AF in specific patient populations.

REFERENCES

1. Verma A, Jiang C, Betts TR, et al. Approaches to catheter ablation for persistent atrial fibrillation. N Engl J Med 2015;372:1812–22.

2. Wong KCK, Paisey JR, Sopher M, et al. No benefit of complex fractionated atrial electrogram ablation in addition to circumferential pulmonary vein ablation and linear ablation: Benefit of Complex Ablation Study. Circ Arrhythm Electrophysiol 2015;8:1316–24.

3. Oral H, Chugh A, Good E, et al. Radiofrequency catheter ablation of chronic atrial fibrillation guided by complex electrograms. Circulation 2007;115:2606–12.

4. Providência R, Lambiase PD, Srinivasan N, et al. Is there still a role for complex fractionated atrial electrogram ablation in addition to pulmonary vein isolation in patients with paroxysmal and persistent atrial fibrillation? Meta-analysis of 1415 patients. Circ Arrhythm Electrophysiol 2015;8:1017–29.

5. Vogler J, Willems S, Sultan A, et al. Pulmonary vein isolation versus defragmentation: the CHASE-AF clinical trial. J Am Coll Cardiol 2015;66:2743–52.

6. Nademanee K, McKenzie J, Kosar E, et al. A new approach for catheter ablation of atrial fibrillation: mapping of the electrophysiologic substrate. J Am Coll Cardiol 2004;43:2044–53.

7. Seitz J, Horvilleur J, Curel L, et al. Active or passive pulmonary vein in atrial fibrillation: is pulmonary vein isolation always essential? Heart Rhythm 2014;11:579–86.

8. Seitz J, Bars C, Ferracci A, et al. Electrogram fractionation-guided ablation in the left atrium decreases the frequency of activation in the pulmonary veins and leads to atrial fibrillation termination. J Am Coll Cardiol EP 2016;2:732–42.

9. Jaïs P, Haïssaguerre M, Shah DC, Chouairi S, Clémenty J. Regional disparities of endocardial atrial activation in paroxysmal atrial fibrillation. Pacing Clin Electrophysiol 1996;19:1998–2003.

10. Rostock T, Rotter M, Sanders P, et al. High-density activation mapping of fractionated electrograms in the atria of patients with paroxysmal atrial fibrillation. Heart Rhythm 2006;3:27–34.

11. Narayan SM, Wright M, Derval N, et al. Classifying fractionated electrograms in human atrial fibrillation using monophasic action potentials and activation mapping: evidence for localized drivers, rate acceleration, and nonlocal signal etiologies. Heart Rhythm 2011;8:244–53.

12. Ganesan P, Cherry EM, Pertsov AM, Ghoraani B. Characterization of electrograms from multipolar diagnostic catheters during atrial fibrillation. BioMed Res Int 2015;2015:272954.

13. Haïssaguerre M, Hocini M, Sanders P, et al. Localized sources maintaining atrial fibrillation organized by prior ablation. Circulation 2006;113:616–25.

14. Narayan SM, Krummen DE, Shivkumar K, Clopton P, Rappel W-J, Miller JM. Treatment of atrial fibrillation by the ablation of localized sources: CONFIRM (Conventional Ablation for Atrial Fibrillation With or Without Focal Impulse and Rotor Modulation) trial. J Am Coll Cardiol 2012;60:628–36.

15. Haissaguerre M, Hocini M, Denis A, et al. Driver domains in persistent atrial fibrillation. Circulation 2014;130:530–8.

16. Scherr D, Khairy P, Miyazaki S, et al. Five-year outcome of catheter ablation of persistent atrial fibrillation using termination of atrial fibrillation as a procedural endpoint. Circ Arrhythm Electrophysiol 2015;8:18–24.

17. Seitz J, Horvilleur J, Lacotte J, et al. Automated detection of complex fractionated atrial electrograms in substrate-based atrial fibrillation ablation: better discrimination with a new setting of CARTO® algorithm. J Atr Fibrillation 2013;2:16–21.

18. Jadidi AS, Lehrmann H, Keyl C, et al. Ablation of persistent atrial fibrillation targeting low-voltage areas with selective activation characteristics. Circ Arrhythm Electrophysiol 2016;9:e002962.

19. Kalifa J, Tanaka K, Zaitsev AV, et al. Mechanisms of wave fractionation at boundaries of high-frequency excitation in the posterior left atrium of the isolated sheep heart during atrial fibrillation. Circulation 2006;113:626–33.

20. Spach MS, Dolber PC, Heidlage JF. Influence of the passive anisotropic properties on directional differences in propagation following modification of the sodium conductance in human atrial muscle. A model of reentry based on anisotropic discontinuous propagation. Circ Res 1988;62:811–32.

21. Atienza F, Calvo D, Almendral J, et al. Mechanisms of fractionated electrograms formation in the posterior left atrium during paroxysmal atrial fibrillation in humans. J Am Coll Cardiol 2011;57:1081–92.

22. Sanders P, Berenfeld O, Hocini M, et al. Spectral analysis identifies sites of high-frequency activity maintaining atrial fibrillation in humans. Circulation 2005;112:789–97.

23. Atienza F, Almendral J, Jalife J, et al. Real-time dominant frequency mapping and ablation of dominant frequency sites in atrial fibrillation with left-to-right frequency gradients predicts long-term maintenance of sinus rhythm. Heart Rhythm 2009;6:33–40.

24. Tanaka K, Zlochiver S, Vikstrom KL, et al. Spatial distribution of fibrosis governs fibrillation wave dynamics in the posterior left atrium during heart failure. Circ Res 2007;101:839–47.

25. Ashihara T, Haraguchi R, Nakazawa K, et al. The role of fibroblasts in complex fractionated electrograms during persistent/permanent atrial fibrillation: implications for electrogram-based catheter ablation. Circ Res 2012;110:275–84.

26. Jadidi AS, Cochet H, Shah AJ, et al. Inverse relationship between fractionated electrograms and atrial fibrosis in persistent atrial fibrillation: combined magnetic resonance imaging and high-density mapping. J Am Coll Cardiol 2013;62:802–12.

27. Akoum N, Wilber D, Hindricks G, et al. MRI assessment of ablation-induced scarring in atrial fibrillation: analysis from the DECAAF study. J. Cardiovasc Electrophysiol 2015;26:473–80.

28. Akoum N, Daccarett M, McGann C, et al. Atrial fibrosis helps select the appropriate patient and strategy in catheter ablation of atrial fibrillation: a DE-MRI guided approach. J Cardiovasc Electrophysiol 2011;22:16–22.

KEY WORDS cycle length, dispersion driver, fractionated, mapping, sinus rhythm

APPENDIX For an expanded Methods section as well as supplemental figures, tables, and videos with legends, please see the online version of this article.